REPORT DOCUMENTATION PAGE

Form Approved
OMB No. 0704-0188

1. REPORT DATE *(DD-MM-YYYY)*	2. REPORT TYPE	3. DATES COVERED *(From - To)*
29-07-2010	Journal Article	

4. TITLE AND SUBTITLE
Cycle of Vertical and Horizontal Mixing in a Shallow Tidal Creek

5a. CONTRACT NUMBER

5b. GRANT NUMBER

5c. PROGRAM ELEMENT NUMBER
0602435N

6. AUTHOR(S)
Paul McKay and Daniela Di Iorio

5d. PROJECT NUMBER

5e. TASK NUMBER

5f. WORK UNIT NUMBER
73-6263-09-5

7. PERFORMING ORGANIZATION NAME(S) AND ADDRESS(ES)
Naval Research Laboratory
Oceanography Division
Stennis Space Center, MS 39529-5004

8. PERFORMING ORGANIZATION REPORT NUMBER
NRL/JA/7320--09-9369

9. SPONSORING/MONITORING AGENCY NAME(S) AND ADDRESS(ES)
Office of Naval Research
800 N. Quincy St.
Arlington, VA 22217-5660

10. SPONSOR/MONITOR'S ACRONYM(S)
ONR

11. SPONSOR/MONITOR'S REPORT NUMBER(S)

12. DISTRIBUTION/AVAILABILITY STATEMENT
Approved for public release, distribution is unlimited.

13. SUPPLEMENTARY NOTES

20100820120

14. ABSTRACT

An experimental study of vertical mixing and along-channel dispersion parameterized in terms of horizontal mixing near the mouth of the Duplin River (a tidal creek bordered by extensive intertidal salt marshes on Sapelo Island, Georgia) was carried out over several spring/neap cycles in the fall of 2005. Vertical mixing is modulated on both M4 and fortnightly frequencies with maximum turbulent stresses being generated near the bed on periods of maximum flood and ebb and propagating into the water column showing a linear dependence with depth. Values are significantly greater on spring tide than on neap. Horizontal mixing evaluated by salt fluxes is driven and dominated by tidal dispersion, which is also modulated by the fortnightly spring/neap cycle. Net export of salt from the lower Duplin is shown to be due to residual advection modified by upstream tidal pumping. The tidal dispersion coefficient exhibits a pulsating character with greater values on spring tide followed by smaller values on neap tide.

15. SUBJECT TERMS
tidal dispersion, vertical mixing, estuary

16. SECURITY CLASSIFICATION OF:			17. LIMITATION OF ABSTRACT	18. NUMBER OF PAGES	19a. NAME OF RESPONSIBLE PERSON
a. REPORT	b. ABSTRACT	c. THIS PAGE			Paul McKay
Unclassified	Unclassified	Unclassified	UL	16	19b. TELEPHONE NUMBER *(Include area code)* 228-688-5664

PUBLICATION OR PRESENTATION RELEASE REQUEST

Pubkey: 6321 NRLINST 5600.2

1. REFERENCES AND ENCLOSURES	2. TYPE OF PUBLICATION OR PRESENTATION		3. ADMINISTRATIVE INFORMATION
Ref: (a) NRL Instruction 5600.2 (b) NRL Instruction 5510.40D Encl: (1) Two copies of subject paper (or abstract)	( ) Abstract only, published ( ) Book ( ) Conference Proceedings (refereed) ( ) Invited speaker (X) Journal article (refereed) ( ) Oral Presentation, published ( ) Other, explain	( ) Abstract only, not published ( ) Book chapter ( ) Conference Proceedings (not refereed) ( ) Multimedia report ( ) Journal article (not refereed) ( ) Oral Presentation, not published	STRN NRLJA/7320-09-9369 Route Sheet No. 7320/ Job Order No. 73-6263-09-5 Classification X U ___ C Sponsor ONR approval obtained ___ yes X no

4. AUTHOR

Title of Paper or Presentation

~~The~~ Cycle of Vertical and Horizontal Mixing In a Shallow Tidal Creek

Author(s) Name(s) (*First,MI,Last), Code, Affiliation if not NRL*

Paul McKay, Daniela Di Iorio

It is intended to offer this paper to the _____
(*Name of Conference*)

(*Date, Place and Classification of Conference*)

and/or for publication in **Journal of Geophysical Research, Unclassified**
(*Name and Classification of Publication*) (*Name of Publisher*)

After presentation or publication, pertinent publication/presentation data will be entered in the publications data base, in accordance with reference (a).
It is the opinion of the author that the subject paper (is ____) (is not ___X) classified, in accordance with reference (b).
This paper does not violate any disclosure of trade secrets or suggestions of outside individuals or concerns which have been communicated to the Laboratory in confidence. This paper (does ____) (does not ___X) contain any militarily critical technology.
This subject paper (has ____) (has never __X__) been incorporated in an official NRL Report.

Paul McKay
Name and Code (*Principal Author*) (Signature)

5. ROUTING/APPROVAL

CODE	SIGNATURE	DATE	COMMENTS
Author(s) McKay		9/11/2009	Need by 28 Sep 09
			Publicly accessible sources used for this publication
Section Head Allard		9/11/09	
Branch Head **Gregg A. Jacobs, 7320**		9-14-09	
Division Head **Ruth H. Preller, 7300**		9/14/09	1. Release of this paper is approved. 2. To the best knowledge of this Division, the subject matter of this paper (has ____) (has never __X__) been classified.
Security, Code **1226**			1. Paper or abstract was released. 2. A copy is filed in this office.
Office of Counsel,Code **1008.3**		11/30/09	
ADOR/Director NCST **E. R. Franchi, 7000**			
Public Affairs *(Unclassified/ Unlimited Only)*, Code **7030.4**	Shannon Boeland	11/30/09	
Division, Code			
Author, Code			

PUBLICATION OR PRESENTATION RELEASE REQUEST 09-1226-3332

1. REFERENCES AND ENCLOSURES	2. TYPE OF PUBLICATION OR PRESENTATION		3. ADMINISTRATIVE INFORMATION
Ref: (a) NRL Instruction 5600.2 (b) NRL Instruction 5510.40D	( ) Abstract only, published ( ) Book ( ) Conference Proceedings (refereed)	( ) Abstract only, not published ( ) Book chapter ( ) Conference Proceedings (not refereed)	STRN NRL/JA/7320-09-9369 Route Sheet No. 7320/
Encl: (1) Two copies of subject paper (or abstract)	( ) Invited speaker (X) Journal article (refereed) ( ) Oral Presentation, published ( ) Other, explain	( ) Multimedia report ( ) Journal article (not refereed) ( ) Oral Presentation, not published	Job Order No. 73-6263-09-5 Classification X U Sponsor ONR 9-6-2 approval obtained ___ yes X no

AUTHOR

Title of Paper or Presentation

Tidal Cycle of Vertical and Horizontal Mixing in a Shallow Tidal Creek

Author(s) Name(s) (*First,MI,Last*), Code, *Affiliation if not NRL*

Paul McKay, Daniela Di Iorio

It is intended to offer this paper to the _____
(Name of Conference)

_____
(Date, Place and Classification of Conference)

and/or for publication in **Journal of Geophysical Research, Unclassified** _____
(Name and Classification of Publication) *(Name of Publisher)*

After presentation or publication, pertinent publication/presentation data will be entered in the publications data base, in accordance with reference (a).
It is the opinion of the author that the subject paper (is ____) (is not X) classified, in accordance with reference (b).
This paper does not violate any disclosure of trade secrets or suggestions of outside individuals or concerns which have been communicated to the Laboratory in confidence. This paper (does ____) (does not X) contain any militarily critical technology.
This subject paper (has ____) (has never X) been incorporated in an official NRL Report.

Contractor Paul McKay (Signature)
Name and Code *(Principal Author)*

ROUTING/APPROVAL

CODE	SIGNATURE	DATE	COMMENTS
Author(s) McKay		9/1/2009	Need by 28 Sep 09
			Publicly accessible sources used for this publication
Section Head Allard	Richard Allard	9/11/09	This is a Final Security Review. Any changes made in the document after approved by Code 1226 nullify the Security Review
Branch Head Gregg A. Jacobs, 7320		9-14-09	1. Release of this paper is approved. 2. To the best knowledge of this Division, the subject matter of this paper (has ____) (has never X) been classified.
Division Head Ruth H. Preller, 7300		9/14/09	
Security, Code 1226		9/17/09	1. Paper or abstract was released. 2. A copy is filed in this office.
Office of Counsel,Code 1008.3		11/30/09	Sponsor Approval Attached
ADOR/Director NCST E. R. Franchi, 7000			
Public Affairs *(Unclassified/ Unlimited Only)*, Code 7030.4	Shannon Boland	11/30/09	Personally identifying email addresses may not be posted to publicly accessible DON websites per SECNAVINST 5720.47B, encl. (1), 3.d.(7)
Division, Code			del Email
Author, Code			SEP 17

HQ-NRL 5511/6 (Rev. 12-86) (e) THIS FORM CANCELS AND SUPERSEDES ALL PREVIOUS VERSIONS

JOURNAL OF GEOPHYSICAL RESEARCH, VOL. 115, C01004, doi:10.1029/2008JC005204, 2010

Cycle of vertical and horizontal mixing in a shallow tidal creek

Paul McKay[1,2] and Daniela Di Iorio[1]

Received 19 November 2008; revised 25 August 2009; accepted 8 September 2009; published 14 January 2010.

[1] An experimental study of vertical mixing and along-channel dispersion parameterized in terms of horizontal mixing near the mouth of the Duplin River (a tidal creek bordered by extensive intertidal salt marshes on Sapelo Island, Georgia) was carried out over several spring/neap cycles in the fall of 2005. Vertical mixing is modulated on both M4 and fortnightly frequencies with maximum turbulent stresses being generated near the bed on periods of maximum flood and ebb and propagating into the water column showing a linear dependence with depth. Values are significantly greater on spring tide than on neap. Horizontal mixing evaluated by salt fluxes is driven and dominated by tidal dispersion, which is also modulated by the fortnightly spring/neap cycle. Net export of salt from the lower Duplin is shown to be due to residual advection modified by upstream tidal pumping. The tidal dispersion coefficient exhibits a pulsating character with greater values on spring tide followed by smaller values on neap tide.

Citation: McKay, P., and D. Di Iorio (2010), Cycle of vertical and horizontal mixing in a shallow tidal creek, *J. Geophys. Res.*, *115*, C01004, doi:10.1029/2008JC005204.

1. Introduction

[2] Efforts to understand the nature of the transfer of materials and dissolved substances across the land-ocean boundary, and into the coastal ocean, must necessarily focus on the estuaries and tidal creeks where such fluxes are concentrated. Since the early work on estuarine dynamics [see, e.g., *Pritchard*, 1952, 1954; *Hansen and Rattray*, 1965] vertical mixing, largely driven by bottom stress, surface stress and internally generated turbulence, has been known to be an important control on the salt flux through its action on vertical stratification. More recently the spring-neap cycle, with its attendant modulation of tidal energy, has come to be appreciated as an important control on this vertical mixing itself [see, e.g., *Peters*, 1997; *Chant*, 2002; *Simpson et al.*, 2005; *Chant et al.*, 2007].

[3] Longitudinal salt fluxes are the result of both advective and dispersive processes [*Dyer*, 1997], with the advective fluxes due, primarily, to fresh water input at the head and the dispersive fluxes due to gravitational circulation and tidal processes, and thus maximum near the mouth of an estuary or tidal creek [*Geyer and Signell*, 1992]. These longitudinal fluxes can vary greatly on seasonal and spring/neap time scales, with changes in fresh water input and tidal energy making them difficult to predict [see, e.g., *Banas et al.*, 2004; *Medeiros and Kjerfve*, 2005].

[4] This paper presents the results of a experiment conducted over several spring/neap cycles near the mouth of the Duplin River, a salt marsh tidal creek on the central Georgia coast. The objective of this study is to quantify the influence of the spring/neap cycle on both vertical mixing and longitudinal dispersion, which can be viewed as horizontal mixing, with the aim of better understanding the relative importance of the down estuary flux by freshwater flow and the up-estuary flux by dispersive processes. The mean properties of the Duplin have been previously reported on [see, e.g., *Ragotzkie and Bryson*, 1955; *Kjerfve*, 1973; *Imberger et al.*, 1983] but this is the first study in this region to look at both horizontal and vertical mixing over spring/neap time scales, processes that are important for controlling the distribution and dilution of salinity. As tidal mixing is strong in this shallow estuary (as will be shown), it is expected that any stratification induced by straining processes will have a negligible effect and thus we classify this estuary as well mixed.

[5] The study site is a tidal creek located in the marshes of the Sapelo Island National Estuarine Research Reserve on the central Georgia coast in the southeastern U.S. (see Figure 1). The Duplin is approximately 13 km long, three times the estimated tidal excursion distance [*Ragotzkie and Bryson*, 1955], and varies from less than 1 m wide at its head, in the intertidal marsh, to 200 m wide at its mouth. It connects with Doboy Sound, which in turn is connected to the coastal Atlantic Ocean. The upper reaches of the Duplin wind through extensive intertidal marshes characterized by mud flats, vegetated primarily with *Spartina alterniflora* and cut by a network of side creeks and channels of varying sizes, while the lower reaches consist of a straight and wide channel with few side creeks bordered by more upland, marsh hammocks and creekless marsh.

[6] The mean depth along the thalweg in the lower Duplin is approximately 6.5 m. The drainage area of the intertidal marsh is approximately 12 km^2 [*Blanton et al.*, 2007]. Tidal flows are ebb dominant and this is a common characteristic of this class of salt marsh estuary [*Dronkers*,

[1]Department of Marine Science, University of Georgia, Athens, Georgia, USA.
[2]Now at Naval Research Laboratory, Stennis Space Center, Mississippi, USA.

0148-0227/10/2008JC005204$09.00

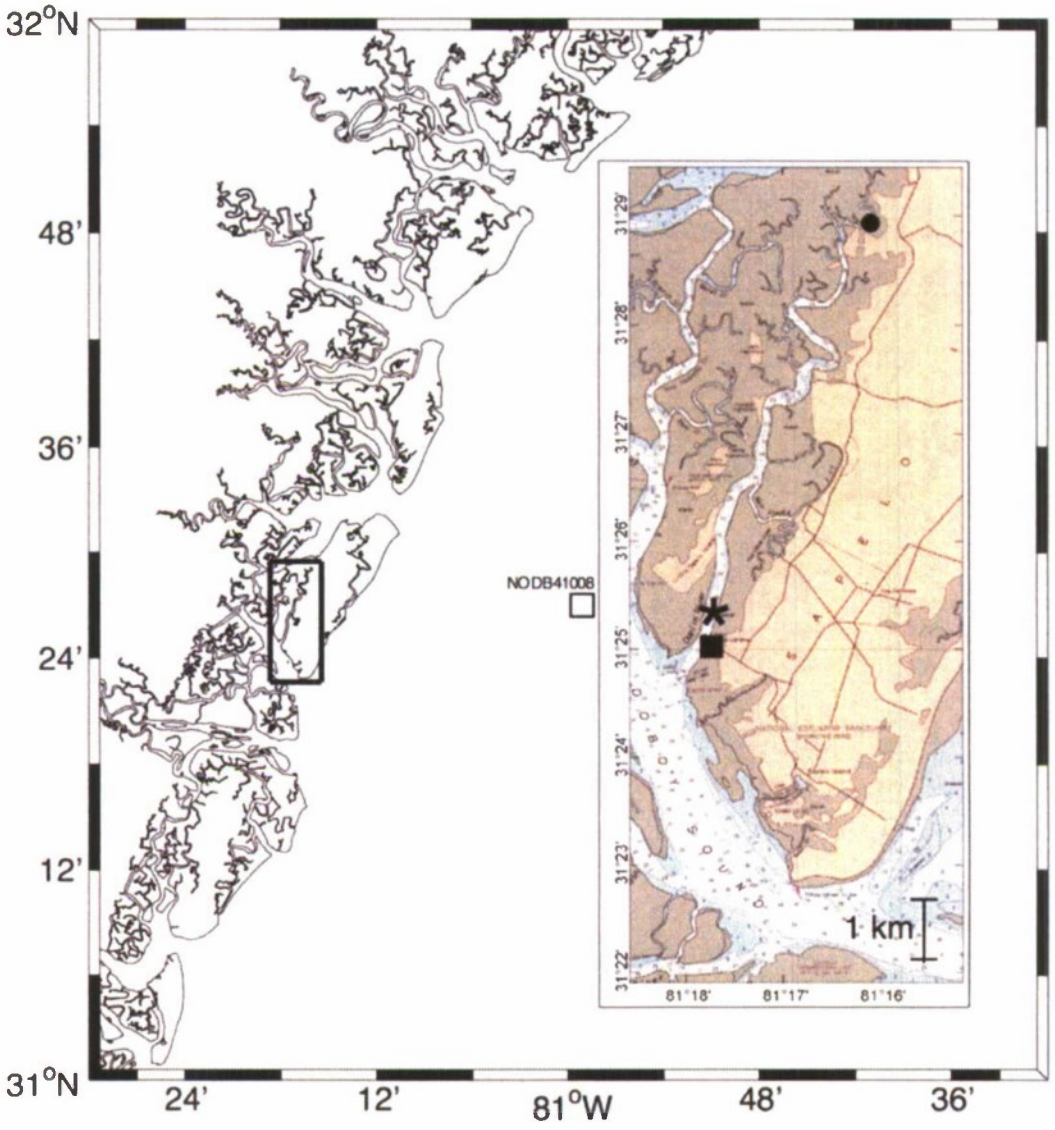

Figure 1. Chart showing the study area on the central Georgia coast showing the ADCP mooring in the lower Duplin (asterisk), the Marsh Landing weather station (solid square), and the GCE-10 site in the upper Duplin (solid circle) where the GCE-LTER project maintains a long-term monitoring station. The offshore National Data Buoy 41008 (open square) provides the offshore wind forcing.

1986; *Dyer*, 1997; *Blanton et al.*, 2002] with a short strong ebb flow and a slower prolonged flood.

[7] The freshwater input in this region is primarily from submarine groundwater input [*Ragotzkie and Bryson*, 1955] with intermittent surface runoff due to precipitation. This input, which is ungauged, establishes an along channel salinity gradient in the lower reaches which can be as much as 2.5 per km or more (as measured using the practical salinity scale) over the length of one tidal excursion. Upstream of this lower section the waters are generally well mixed along the channel and the salinity gradient, when present, is much smaller and variable. There is significant tidal salinity variation in the lower reaches of the Duplin as water from Doboy Sound (influenced by the Altamaha River) is advected by *Kjerfve* [1973]. While there are occasional periods of stratification in the lower Duplin (believed to be related to changes in Altamaha River discharge, groundwater input and precipitation), it is generally vertically and laterally well mixed.

[8] In this paper, section 2 outlines the details of the experiment and data processing and section 3 describes the mathematical framework for vertical and horizontal mixing and dispersion in estuaries. The measured mixing and dispersion results are summarized in section 4 and section 5 discusses implications for a better physical understanding of tidal creek export to the coastal ocean.

2. Experimental Program

[9] Meteorological conditions at the offshore National Data Buoy 41008 station and the Marsh Landing weather station adjacent to the deployment location (see Figure 1)

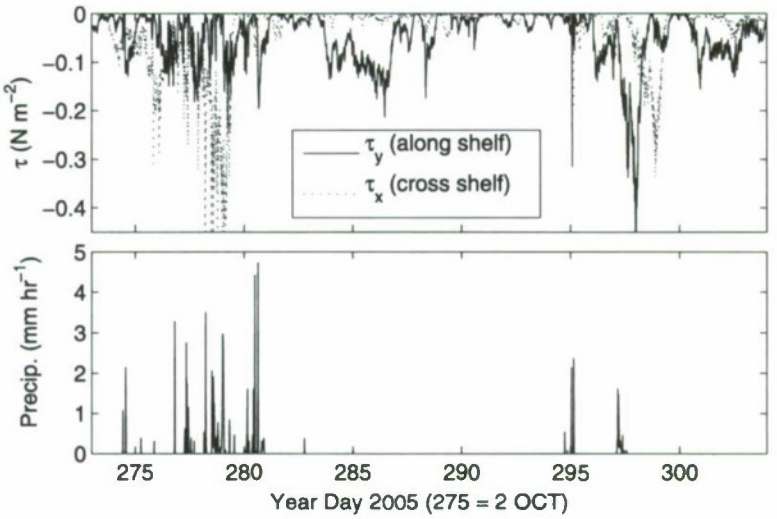

Figure 2. The coastal wind stress in terms of along- (positive is to the north) and cross- (positive is to the east) shelf components showing that during this time of year the winds are predominantly from the northeast. The precipitation rate at the Marsh Landing weather station immediately adjacent to the mooring location are also shown.

are shown in Figure 2. Wind stresses show that the coastal storms are predominately from the northeast which can increase inundation in the estuary through Ekman transport processes (as will be seen in the residual sea level height in Figure 4) Sporadic rain showers were observed on year day 274–281, 295 and 297, and the region had been recovering from a drought in 2001 and 2002. Some of the decrease in mean salinity from year day 278–281 (as will be shown) is

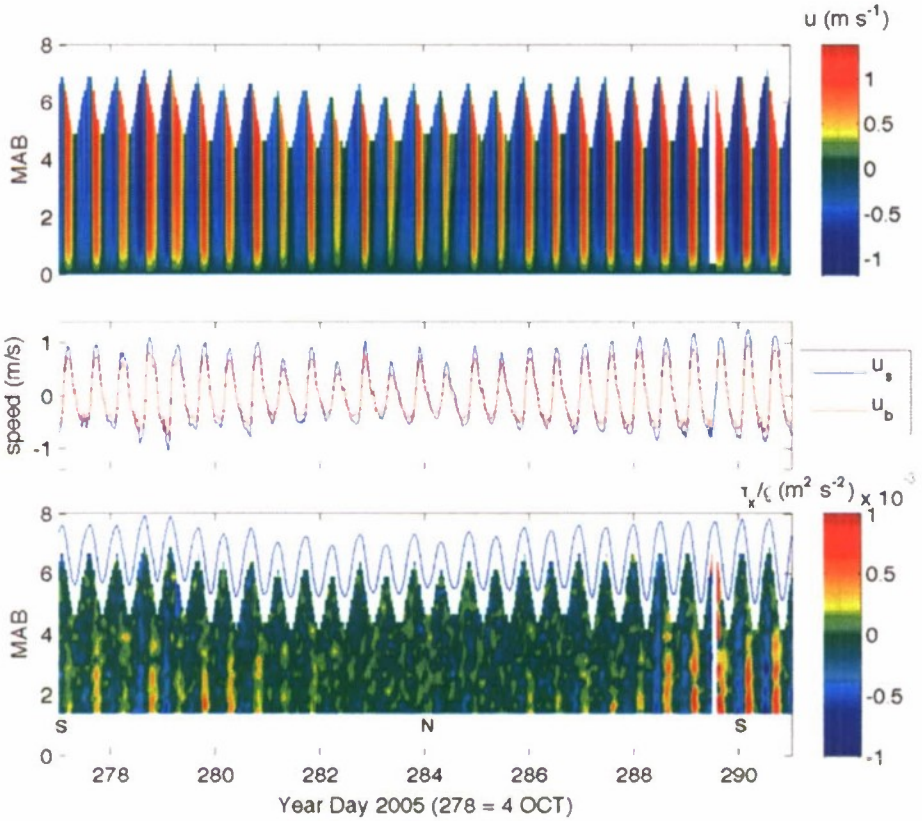

Figure 3. The depth-dependent along-channel velocity (u) is plotted together with the surface and bottom velocities. The Reynold's stress (τ_x/ρ) is shown during a spring-neap-spring period from year day 277–291. Measurements, where indicated, are a function of mab.

likely attributable to this rain event, however this period also corresponds with the spring tide, which is believed to increase fresh groundwater flux into the channel (as will be discussed).

[10] The field experiment in the lower Duplin River was carried out over a 34 day period from 28 September to 31 October 2005 and covered two spring and two neap tides, ending shortly before a third spring tide. Figure 1 shows a hydrographic chart of the study area on the Georgia coast as well as the location of our instruments. The instrument package was deployed during the September 2005 Georgia Coastal Ecosystems (GCE)-Long Term Ecological Research (LTER) survey cruise with the R/V Savannah. A 4 beam 1200 kHz broadband acoustic Doppler current profiler (ADCP) was deployed on a heavy custom built pyramidal bottom mount mooring frame in the center of the channel in water with a mean depth of approximately 6.5 m. The ADCP operated in burst mode, sampling current velocity profiles at 2 Hz for 5 minutes every 30 minutes, and logged every ping in beam coordinate mode with 0.25 m depth bins. The first sample was centered 1.0 m above bottom when taking into account blanking distance. The 1–2 beam pair was aligned along the main axis of the channel.

[11] For each beam, the velocity data at the top bin and bottom two bins were deleted, to remove both surface noise and ringing near the transducer. Each beam was then further processed by removing all ping data with a percent good (PG) of less than 90% as reported by the internal diagnostics of the ADCP. For an ADCP logging every ping this is a measure of the echo strength of the returned signal. This resulted in the removal of one complete five minute ensemble on year day 289 as well as the removal of scattered other values, generally near the surface, which constituted less than 1% of the data. With the exception of the removed ensemble, deleted beam velocities were replaced with a linear interpolation between the values in the bins above and below. Finally, for each depth bin, spikes in the data were rejected that were three or more standard deviations away from the ensemble average and were replaced with an interpolated value. This also removed a small amount of data.

[12] The along channel (u) and cross channel (v) velocities are calculated from the individual ADCP pings as

$$u = \frac{B_2 - B_1}{2\sin\theta}, \qquad v = \frac{B_4 - B_3}{2\sin\theta}, \tag{1}$$

where B_i is the along beam velocity for each beam (i = 1, 2, 3, 4), the 1–2 beam pair is aligned with the channel, the 3–4 beam pair is aligned cross channel and $\theta = 20°$ is the beam angle (for the RDI ADCP used) [*Di Iorio and Gargett*, 2005]. The instantaneous u and v velocities were then averaged for each five minute ensemble to get the mean flow. To resolve the surface and bottom flows each velocity profile was extrapolated to the surface, over a distance of 0.5 m, by assuming zero shear at the surface, and extrapolated to the bottom assuming a log layer profile over a 1.5 m distance.

[13] Compass and pitch/roll sensors show that during this deployment the instrument's heading changed 0.5° over 34 days while pitch and roll started out at less than 3 and 1.5°, respectively, from the vertical with both settling to just over 1° over the first 10 days of the deployment and remaining constant for the rest of the deployment. While stress estimates are very sensitive to instrument alignment with the vertical, *Lu and Lueck* [1999] showed that errors in the stress estimate will be small for such small deviations. Our coordinate system adheres to the estuarine convention such that x is the along channel direction and is positive out of the creek.

[14] Microcat conductivity-temperature-depth (CTD) meters were deployed with the ADCP mooring with a bottom sensor mounted to the ADCP frame approximately 0.5 meters above bottom and a surface sensor attached to a line tethered to a surface marker float and deployed 0.5 m below the surface. In addition the GCE-LTER project maintains a long-term CTD station in the upper Duplin at mid depth. All CTDs sampled at 15 minute intervals. The bottom Microcat salinity data became unreliable, due to biofouling of the sensor, on the fifth day of the deployment. Prior to this instrument failure, the surface and bottom measurements indicated that the system was vertically well mixed for both temperature and salinity at all times with the differences showing a random distribution and being below the noise threshold of each sensor. As this agrees with the authors' observations during two previous mooring experiments at this location in the Duplin River [*McKay and Di Iorio*, 2008] we have chosen to treat the surface values as being indicative of the entire water column. While rain events likely introduced some short-lived stratification to the water column we were not able to measure this. Salinity will be reported as a unitless quantity in accordance to the practical salinity scale adopted in 1978.

3. Methods

3.1. Vertical Mixing

[15] In a sheared flow, vertical mixing results from bottom boundary-induced turbulence or breaking internal waves (Kelvin-Helmholtz instabilities) depending on the strength of the stratification. For the weakly stratified case, *Jay and Smith* [1990] show that when the shear is large enough relative to the stratification then bottom boundary-induced turbulent mixing extends throughout most of the water column and causes vertical exchange of properties. Any tidal asymmetries would then come from the mean flow as the velocities on ebb are greater because the shear and flow speed are augmented by the mean river flow. The barotropic tidal advection of the density field dominates in weakly stratified estuaries, as the gravitational restoring force is weak and therefore baroclinic motions do not exist.

[16] It is common to treat turbulent mixing (vertical flux of horizontal momentum and salt) as a gradient process parameterized against the mean velocity shear and salinity gradient with a vertical eddy viscosity, A_z, and vertical scalar diffusivity, K_z, respectively, (with units of $m^2\ s^{-1}$) such that

$$-\overline{u'w'} = A_z \frac{\partial \bar{u}}{\partial z} \tag{2}$$

$$-\overline{w's'} = K_z \frac{\partial \bar{s}}{\partial z}. \tag{3}$$

The along channel and vertical velocities are u and w, respectively, and the subscript z is the vertical; the overline

represents a time averaged quantity and primed values represent the turbulent fluctuations from the time average [*Dyer*, 1997].

[17] Since the work of *Lohrman et al.* [1990], as elaborated by *Stacey et al.* [1999a, 1999b] and *Lu and Lueck* [1999], it has become common to estimate vertical eddy viscosity (A_z), and hence momentum diffusivity, using a four beam, high-frequency broadband acoustic Doppler current profiler (ADCP). This method, known as the variance method, allows the direct estimation of the Reynolds stress, $\tau_x/\rho = -\overline{u'w'}$, by comparing the velocity variances of opposing pairs of beams. This stress is determined using the relation

$$-\overline{u'w'} = \frac{\overline{B_{2f}^2} - \overline{B_{1f}^2}}{2\sin 2\theta}, \tag{4}$$

where $\overline{B_{1f}^2} = \overline{B_1^2} - \overline{B_1^2}$, B_1 is the velocity along the beam one direction and the subscript f implies fluctuations [*Di Iorio and Gargett*, 2005]. $\overline{B_{2f}^2}$ is similarly defined but opposite from beam one. The vertical viscosity $A_z$is then the ratio between the time varying stress and the observed vertical shear.

[18] In energetic tidal channels having vertically well-mixed conditions and hence a gradient Richardson number tending to 0, the turbulent Prandtl number $A_z/K_z = 0.7$ [*Stacey et al.*, 1999a]. In the presence of stratification, vertical mixing has to act against a density gradient and both the eddy viscosity and diffusivity are reduced. However, as momentum is transferred more readily than mass in such a case, K_z is attenuated more than is A_z and the turbulent Prandtl number increases.

[19] The variance method requires the flow to be horizontally homogeneous such that there is no variation in the turbulent statistics over the separation distance between corresponding bins in each beam pair [*Lu and Lueck*, 1999]. This condition is met by our deployment location being in the middle of the channel in a region of nearly constant cross section. The sampling rate of 2 Hz and vertical bin size of 0.25 m allows us to resolve the smaller eddies in the flow which are involved in vertical momentum transfer [*Rippeth et al.*, 2002]. The 5 minute ensemble time represents a compromise between concerns of instrument battery life, the need for a statistically significant sample size and the need for quasi-stationary conditions during the sample period. With a 2 Hz sampling rate, a 5 minute sampling period (600 samples) provided a statistically significant ensemble average of the velocity as the estimated standard error was low (less than 1 cm/s). In a flow dominated by semidiurnal tides, the 5 min period was also short enough to insure quasi-stationary conditions during the entire ensemble.

[20] Stress profiles were calculated for each ping in the record and then averaged for each five minute ensemble to give one stress profile for each half hour period. The statistical reliability of the Reynolds stress estimates increases with the square root of the number of samples per ensemble according to the relation given by *Williams and Simpson*, [2004]

$$\sigma_R^2 = \frac{\gamma\left(\sigma_n^2 - \overline{B_{if}^2}\right)^2}{N\sin^2 2\theta}, \tag{5}$$

where σ_R^2 is the mean squared variability of the Reynolds stress estimate, γ is a factor depending on the covariance of the individual velocity values, σ_n is the instrument noise level, $\overline{B_{if}^2}$ the mean square value of the turbulent fluctuations and N is the number of samples per ensemble. From equation (5) and following the method of *Williams and Simpson* [2004], we can estimate a threshold value for detectable stress by examining low flow, when B_{if} goes to zero and γ to one, and taking a value for instrument noise of $\sigma_n = 0.017$ m s^{-1} from the instrument manufacturer. This then gives an approximate theoretical minimum measurable stress $\tau/\rho = 2 \times 10^{-5}$ m^2 s^{-2}.

[21] To estimate the vertical eddy viscosity, A_z, it is necessary to compute the vertical shear in the along channel velocity, $\partial\overline{u}/\partial z$, in the region where stresses are resolved by the ADCP. As small variations in $\overline{u}$ between depth bins can cause large swings in the value of $\partial\overline{u}/\partial z$, as calculated using numerical differentiation techniques, each velocity profile was smoothed by fitting with a polynomial and the gradient taken by differentiating that polynomial. As the shape of the velocity profile changes through the tidal cycle from being nearly linear to showing slight curvature, each profile was fit with both first and second-order polynomials; the fit with the highest r^2 value was selected for the differentiation. The velocity profile was generally linear with a maximum at the surface.

[22] The vertical mixing time during the tidal cycle is estimated from a tidal and depth average of the vertical mixing quantity K_z [*Lewis*, 1997], as

$$t = \frac{H^2}{8\left\langle \widehat{K_z} \right\rangle} \approx \frac{H^2}{8\left\langle \widehat{A_z} \right\rangle}, \tag{6}$$

where t is the approximate time for complete vertical mixing (in seconds), H the tidal mean water depth, and $\langle\rangle$ denotes tidal averaging and $\widehat{\cdot}$ denotes depth averaging. A turbulent Prandtl scaling of 1 ($K_z \sim A_z$) is assumed and that it is considered stationary within each tidal period. This estimated mixing time is based on the estimated time required for a concentrated substance in the middle of the water column to assume a Gaussian concentration distribution with depth.

3.2. Decomposition of Salt Fluxes

[23] Along channel horizontal mixing in an estuary is a result of the sum of several processes on widely distributed spatial and temporal scales: from turbulent to tidal and fortnightly scales. The interaction between estuarine tides, bathymetry and irregularities at the channel edge can result in dispersive fluxes that are due to tidal pumping/trapping, vertical and lateral shear dispersion, and the estuarine circulation [*Fischer et al.*, 1979]. Of these mechanisms tidal dispersion, the generally upstream net transport due to correlations between tidal depth, velocity and salinity, is often dominant in well mixed estuaries [*Kjerfve*, 1986]. The presence of vertical shear and stratification [*Bowden*, 1965] and a generally much smaller effect of lateral shear and salinity variability [*Rattray and Dworski*, 1980] can act to modulate this tidal pumping mechanism, especially in areas of high stratification or curvature in the main tidal channel [*Dyer*, 1974]. Irregularities in the channel edge, side creeks, and intertidal flats can also contribute to along channel

dispersion by holding water inundated on flood and not releasing it back into the main channel on the following ebb, effectively trapping the water, and returning it back as a different water mass on subsequent ebb tides [*Fischer*, 1976].

[24] As shown in Figure 1, our deployment in the lower Duplin is in an area having a relatively straight channel with few side creeks or irregularities. The width of the channel is approximately $B = 200$ m with the eastern side approximately 1 m deeper than the western side with steep sloping side boundaries. Following the work of *Hansen* [1965] and *Fischer* [1976], as modified by *Medeiros and Kjerfve* [2005], we quantify the cross-sectionally integrated and tidally averaged salt flux as

$$\frac{\partial \langle s^V \rangle}{\partial t} + \frac{1}{A}\int_A \langle aus \rangle da = 0, \tag{7}$$

where the superscript V implies a volume integration of the salinity from the head of the creek where the salt fluxes are zero to the measurement location. We decompose the cross sectional area (a), current velocity (u) and salinity (s) in terms of quantities that describe the residual flow, estuarine circulation (E), tidal variability (t), vertical shear dispersion (V) and lateral shear dispersion (T),

$$u(y,z,t) = U(z) + U_E(z) + u_t(t) + U_V(z,t) + U_T(y,t), \tag{8}$$

$$a(t) \simeq (H(t) + h_t(t))B, \tag{9}$$

$$s(y,z,t) = S(t) + S_E(z) + s_t(t) + S_V(z,t) + S_T(y,t), \tag{10}$$

where the cross sectional area varies according to tidal height and

$$\left\langle \widetilde{\widehat{u}} \right\rangle = \widehat{U} = U_r,\ \widehat{U}_E = 0, \tag{11}$$

$$u_t = \widetilde{\widehat{u}} - \left\langle \widetilde{\widehat{u}} \right\rangle, \tag{12}$$

$$U_V = \langle \widetilde{u} \rangle - \left\langle \widetilde{\widehat{u}} \right\rangle, \tag{13}$$

$$U_T = \langle \widehat{u} \rangle - \left\langle \widetilde{\widehat{u}} \right\rangle. \tag{14}$$

The quantity U_r represents the mean river flow, $\widehat{\ }$ represents a laterally averaged quantity and $\langle u_t \rangle = \widehat{U}_V = \widetilde{U}_T = 0$. Similar equations can be written for the salinity.

[25] As the instrumentation was located in the center of the channel and the bottom salinity measurement was fouled early in the measurement program there is no quantitative measurement of $U_T(y, t)$, and $s(y, z)$. As a result we cannot quantify lateral variations in the longitudinal fluxes but we expect them to be small in such a narrow channel with steep sloping sides and so lateral homogeneity is assumed. In order to quantify estuarine circulation, and the vertical and transverse quantities we make use of steady state formulae. From the energetics of mixing (as will be shown below) it is expected that tidal stirring (mixing) which destroys stratification is much greater than stratification created by the estuarine circulation and tidal straining, and thus we can assume that the lower Duplin during our measurement program is vertically well mixed for most of the tidal cycle. Substituting equations (8) to (10) into (7), we can thus write the salt flux per unit width of the estuary as

$$\frac{1}{B}\frac{\partial \langle s^V \rangle}{\partial t} + \frac{1}{H}\int_{-H}^{0}\Big[HUS + HU_E S_E + H\langle U_V S_V \rangle + \frac{H}{B}\int_{-b}^{b}\langle U_T S_T \rangle dy + H\langle u_t s_t \rangle + U\langle h_t s_t \rangle + S\langle h_t u_t \rangle + \langle h_t u_t s_t \rangle\Big]dz = 0. \tag{15}$$

[26] The first term of equation (15) is the storage of salt per unit width, which accounts for changes in salinity and storage volume. The first term within the integral (HUS) represents the advection of salt due to tidally averaged residual flows reflecting changes in freshwater discharge, mean depth and offshore forcing. The next term is the net transport of salt upstream because of the estuarine circulation that moves freshwater down stream near the surface and salt water upstream at depth. The next two terms are the vertical and transverse shear dispersion. The next set of terms remaining account for the longitudinal tidal dispersive transport due to correlations between tidally varying quantities and correspond to tidal velocity-salinity transport, tidal salinity transport, tidal wave transport (Stoke's drift which is maximum when the tide resembles a progressive wave and is zero for a standing wave) and the tidal pumping transport. Rewriting equation (15) as

$$\frac{1}{B}\frac{\partial \langle S^V \rangle}{\partial t} + HU_r S = -\int_{-H}^{0}[U_E S_E + \langle U_V S_V \rangle]dz - \frac{H}{B}\int_{-b}^{b}\langle U_T S_T \rangle dy - [H\langle u_t s_t \rangle + U_r\langle h_t s_t \rangle + S\langle h_t u_t \rangle + \langle h_t u_t s_t \rangle] \tag{16}$$

$$= HK_x\frac{\partial S}{\partial x}. \tag{17}$$

The dispersive flux terms can then be parameterized against the along channel salinity gradient, $\partial S/\partial x$, to obtain an effective along channel dispersion coefficient, K_x.

3.2.1. Estuarine Circulation

[27] The governing equations that describe the residual flow in steady state are

$$0 = -g\frac{\partial \eta}{\partial x} + \frac{g}{\rho}\frac{\partial \rho}{\partial x}z + A_z\frac{\partial^2 u}{\partial z^2} \tag{18}$$

$$U_E\frac{\partial S}{\partial x} = K_z\frac{\partial^2 S_E}{\partial z^2}, \tag{19}$$

where it is assumed to a first-order approximation that A_z and $\partial\rho/\partial x$ are constant with depth. The barotropic pressure gradient associated with the sea surface slope ($\partial\eta/\partial x$) drives the fresh water out on top and the baroclinic pressure gradient associated with the along channel density gradient ($\partial\rho/\partial x$) drives the ocean flow in at depth.

[28] Integrating (18) twice with respect to z and applying the boundary conditions that there is no stress at the surface ($A_z\partial u/\partial z|_{z=0} = 0$) and no flow at the bottom ($u(z = -H) = 0$) gives

$$u = \frac{g}{A_z}\left(\frac{1}{2}\frac{\partial \eta}{\partial x}(z^2 - H^2) - \frac{1}{6\rho}\frac{\partial \rho}{\partial x}(z^3 + H^3)\right). \quad (20)$$

To find the sea surface slope the river outflow is defined as $\int_{-H}^{0} u dz = HU_r$ and as such the depth-dependent residual flow is

$$u = \frac{g}{\rho}\frac{\partial \rho}{\partial x}\frac{H^3}{48A_z}\left(1 - 9\left(\frac{z}{H}\right)^2 - 8\left(\frac{z}{H}\right)^3\right) + \frac{3}{2}U_r\left(1 - \left(\frac{z}{H}\right)^2\right) \quad (21)$$

$$= U_E(z) + U(z), \quad (22)$$

where the first term on the right is the estuarine velocity and the second term on the right is the river velocity.

[29] Substituting the estuarine velocity U_E into (19), integrating twice with respect to z, applying the boundary conditions of no flux out of the sea surface ($A_z\partial S_E\partial z|_{z=0} = 0$) and that $\int_{-H}^{0} S_E dz = 0$ gives the following estuarine salinity (for $K_z \sim A_z$):

$$S_E = \frac{g}{\rho}\frac{\partial \rho}{\partial x}\frac{\partial S}{\partial x}\frac{H^5}{48A_z^2}\left(-\frac{1}{12} + \frac{1}{2}\left(\frac{z}{H}\right)^2 - \frac{3}{4}\left(\frac{z}{H}\right)^4 - \frac{2}{5}\left(\frac{z}{H}\right)^5\right). \quad (23)$$

The depth integrated salt flux due to the estuarine circulation is then

$$\int_{-H}^{0} U_E S_E dz = -\frac{19}{630}\left(\frac{g}{48\rho}\frac{\partial \rho}{\partial x}\right)^2 \frac{H^9}{A_z^3}\frac{\partial S}{\partial x}, \quad (24)$$

which is relatively constant and always negative implying that there is a net salt flux upstream.

3.2.2. Vertical Shear

[30] *Bowden* [1965] showed how the interaction between stratification and shear in the mean flow can give rise to horizontal shear dispersion. If the velocity profile is modeled as a linear function with depth $u(z, t) = U_o(t)(1 + (z/H))$ then $U_V(z, t) = U_o(t)(1/2 + z/H)$, where the surface current is defined as U_o. The steady state equation to solve is [*Lewis*, 1997]

$$U_V\frac{\partial S}{\partial x} = K_z\frac{\partial^2 S_V}{\partial z^2}, \quad (25)$$

which represents the perturbed state. Integrating with respect to depth twice and applying the boundary conditions of no flux out of the surface ($K_z\partial S_V/\partial z|_{z=0} = 0$) and that $\int_{-H}^{0} S_V\, dz = 0$ gives the salinity (for $K_z \sim A_z$)

$$S_V = U_o\frac{H^2}{A_z}\frac{\partial S}{\partial x}\left(-\frac{1}{24} + \frac{1}{4}\left(\frac{z}{H}\right)^2 + \frac{1}{6}\left(\frac{z}{H}\right)^3\right). \quad (26)$$

The depth integrated and tidally averaged salt flux due to vertical shear is then

$$\int_{-H}^{0} (U_V S_V) dz = -\langle U_o^2\rangle\frac{H^3}{120A_z}\frac{\partial S}{\partial x}, \quad (27)$$

which is also always negative implying a net salt flux upstream.

3.2.3. Transverse Shear

[31] In a similar way the transverse shear dispersion is calculated for a channel flow of $u(y, t) = U_o(t)\,(1 - (y/b)^2)$ where $B = 2b$ is the width of the channel. This gives $U_T(y, t) = U_o(t)(1/3 - (y/b)^2)$. The steady state equation to solve is

$$U_T\frac{\partial S}{\partial x} = K_y\frac{\partial^2 S_T}{\partial y^2}, \quad (28)$$

where K_y is an estimated cross-estuary mixing parameter. Integrating twice with respect to the cross channel and applying the boundary condition of no fluxes in the middle of the channel ($y = 0$) because of symmetry ($K_y\partial S_T/\partial y|_{y=0} = 0$) and that $\int_{-b}^{b} S_T dy = 0$ gives

$$S_T = -U_o\frac{b^2}{K_y}\frac{\partial S}{\partial x}\left(\frac{7}{180} - \frac{1}{6}\left(\frac{y}{b}\right)^2 + \frac{1}{12}\left(\frac{y}{b}\right)^4\right). \quad (29)$$

Thus,

$$\frac{H}{B}\int_{-b}^{b} (U_T S_T) dy = -\langle U_o^2\rangle\frac{8Hb^2}{945K_y}\frac{\partial S}{\partial x}, \quad (30)$$

which is also a net salt flux upstream. The difficulty in this formulation is quantifying the cross channel mixing (K_y).

3.3. Energetics of Mixing

[32] The important processes that can lead to the creation and destruction of stratification in estuaries are from the estuarine circulation, which causes fresh water outflow at the surface and oceanic inflow at depth, tidal straining of the horizontal density field by the vertical current shear, which causes an increase in stratification during ebb tide and damps the turbulence relative to the flood tide [*Simpson*, 1994; *Souza and Simpson*, 1997] and tidal stirring (mixing), which is a percentage of the turbulent kinetic energy production that goes directly into mixing the water column. Stirring due to wind and waves is assumed negligible as the Duplin estuary exists on the back side of a coastal barrier island.

[33] While no stratification was measured at the mooring site during the brief period when both surface and bottom measurements were available, it is possible that some unmeasured stratification existed at later times and this could have an impact on the along channel salt fluxes. Unstratified estuaries are common in the South Atlantic Bight where relatively high tidal energy interacts with relatively low freshwater fluxes to create vertically well mixed conditions [see, e.g., *Verity et al.*, 1993; *Wiegert et al.*, 1999]. Temporary stratification can be introduced into these estuaries through increases in freshwater input at the head, through an increase in river or groundwater input or through runoff due to a rain event, as well as the decrease in tidal energy at neap tide.

While these stratification events are likely to be short-lived they could have an impact on short-term salt fluxes.

[34] The Duplin River has no regular source of freshwater input; its freshwater is supplied primarily through submarine groundwater inputs [*Ragotzkie and Bryson*, 1955] and localized runoff from rain events. The majority of the groundwater input appears to enter the Duplin upstream of the lower tidal excursion [*McKay*, 2008], and as a result the along channel salinity gradient, $\partial S/\partial x$ is confined to the lower Duplin region. In this section, energetics of mixing is used to see if there are times when stratification can be created. The conservation of density and its depth averaged form can be approximated as

$$\frac{\partial \rho}{\partial t} + u\frac{\partial \rho}{\partial x} = -\frac{\partial}{\partial z}\overline{\rho' w'} \tag{31}$$

$$\frac{\partial \hat{\rho}}{\partial t} + \hat{u}\frac{\partial \rho}{\partial x} = 0, \tag{32}$$

assuming no fluxes through the surface and bottom boundary and $\overline{\rho' w'}$ represents the turbulent flux of mass in the vertical. The rate of change of potential energy anomaly is then defined as the difference between the mixed and stratified states [*Simpson et al.*, 1990]

$$\frac{\partial \phi}{\partial t} = \frac{1}{H}\int_{-H}^{0} gz\frac{\partial}{\partial t}(\hat{\rho} - \rho)dz \tag{33}$$

$$= \frac{g}{H}\frac{\partial \rho}{\partial x}\int_{-H}^{0}(u - \hat{u})z\,dz - \frac{\rho_o}{H}R_f\int_{-H}^{0} P\,dz, \tag{34}$$

where $R_f = \Gamma/(\Gamma + 1)$ is the flux Richardson number representing a percentage of the turbulent kinetic energy production (calculated as $P = -\overline{u'w'}\partial\overline{u}/\partial z$) that goes into mixing the water column, creating a sink of turbulent kinetic energy (TKE) defined by $B = (g/\rho_o)\,\overline{\rho' w'}$, and Γ is the mixing efficiency. The first term on the right hand side of (34) represents the straining that can create (positive values on ebb) or destroy (negative values on flood) stratification; the second term represents the destruction of stratification due to mixing as it is always negative.

4. Results

4.1. Tidal and Residual Properties

[35] Figure 3 (top) shows the depth distribution of the along channel velocity u (positive on ebb), and extrapolated to the surface and bottom during a 14 day spring-neap-spring transition at the beginning of the experiment. Along channel velocity profiles are generally linear with a minimum near the bed and a maximum near the surface. Figure 3 (middle) shows the measured near surface (5 meters above bottom (mab)) and bottom (1.5 mab) flow, during this same period. It shows more clearly the spring/neap cycle, the ebb dominance of flow which is a common characteristic of this class of salt marsh estuary [*Dronkers*, 1986; *Dyer*, 1997; *Blanton et al.*, 2002] and gives an indication of the kind of shear in the water column. This shear is responsible for overturning the water column and keeping it essentially well mixed. The entire period of observation is shown in Figure 4, separated into residual (40 hour low-pass filtered shown as a thick line) and tidal components (shown as a thin line) showing the depth averaged quantities for the along channel flow with the residual flow scaled by a factor of 10 in order to show its variability (Figure 4a); showing salinity, which is taken as representative of the entire water column, for the upper and lower Duplin (Figure 4b); and showing the center channel mean and tidally varying depth (Figure 4c).

[36] A strong spring/neap cycle can be seen in both along channel tidal velocity and tidal depth. Strong spring ebb flows peak as high as 1.2 m s^{-1} while weak neap ebb flows are as slow as half of that, and the tidal height ranges from 1 m on neap to 2.6 m on spring tide. The flow is ebb dominant, showing a shorter, stronger ebb which contrasts with a longer but weaker flood. This is due to frictional distortion of the tide, caused by interactions between the main channel and the intertidal areas, which can be expressed by the relationship between the M2 and M4 tidal constituents [*Dyer*, 1997]. Residual water height H shows some inundation that may occur when the along and cross shelf winds are strong.

[37] The tidally varying salinity varies from 5 to 7 and the mean salinity varies between 23 and 28 in the lower Duplin and 18 to 25 in the upper Duplin. The decrease in salinity on year day 280 may correspond to the accumulated precipitation from the rain events shown in Figure 2 that also causes an increased net outflow. This pattern is also seen at the peak of the spring tide on year day 290 where the salinity decreases when there is a net outflow.

[38] The tidally averaged current flow is shown in Figure 5 along with the theoretical estuarine circulation defined in (21) (for a value of $A_z = 1.1 \times 10^{-3}$ m^2/s, $\partial\rho/\partial x = 2.1 \times 10^{-4}$ kg/m^4 and $H = 6.5$ m). The resulting river flow $U_r = .021$ m/s gives the best fit to the measured profile.

4.2. Reynolds Stresses and TKE Production

[39] In Figure 3 (bottom) we show the stress ($\tau_x/\rho = -\overline{u'w'}$) through the water column during the first spring-neap-spring period. Maximum stresses originate near the bed and propagate upward into the water column decreasing in the upper layers. The periods of highest stress are found during the spring tide centered around maximum flood and ebb when the stresses reach as high as $\pm 1.2 \times 10^{-3}$ m^2 s^{-2} near the bed and show an M4 distribution. There is a pronounced tidal asymmetry in the stress production. They are lower on flood than ebb and the stresses on ebb penetrate significantly further into the water column than on flood, due to peak ebb velocities being much higher, though of shorter duration, than flood. At neap tide there is greatly decreased turbulent stress on maximum ebb and flood with consequently less penetration of the stress into the water column. Near slack water, at both spring and neap tides, the stresses are uniformly low and patchy throughout the water column.

[40] Figure 4d shows a time series of τ_x/ρ, centered 1.5 mab, for the entire deployment period. Both fortnightly and semidiurnal variability in stress production are clearly visible with peak stresses during spring tides being much higher than during neap tides, and with the peak stresses during the second spring tide being more than double those during the first. Semidiurnal variability is seen in that peak positive, ebb tide, stresses are significantly higher than peak negative, flood tide, stresses due to the asymmetry in ebb and

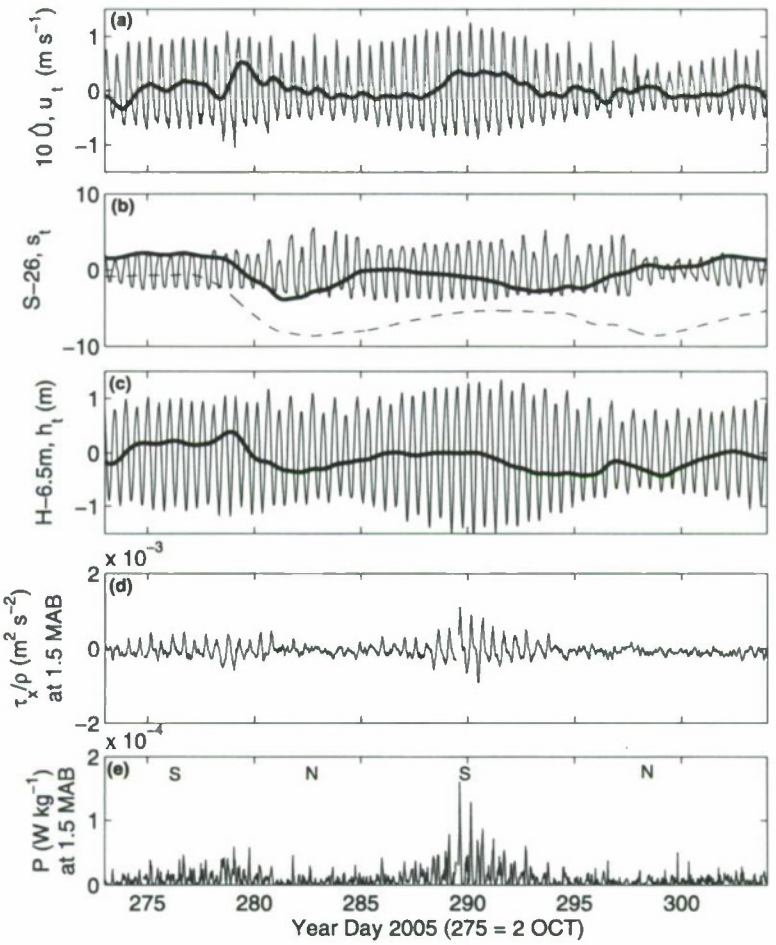

Figure 4. Tidally averaged (40 hour low-pass filtered shown as thick lines) and tidally varying (shown as thin lines) quantities for (a) depth averaged along channel velocity ($\hat{U}$ is scaled by a factor of 10), (b) surface salinity for the lower (solid line) and upper (dashed line) Duplin, and (c) center channel water depth. (d) The Reynolds stress τ_x/ρ and (e) the TKE production (P) both at 1.5 mab are shown together with spring (S) and neap (N) tide labels.

flood velocities. Cross channel stresses, $\tau_y/\rho = -\overline{v'w'}$, are not shown in these plots as they are uniformly low, owing to the low cross channel velocity.

[41] Figure 4e also shows the turbulent kinetic energy production (P) at 1.5 mab. The depth variability (not shown) mirrors the stress distribution as the velocity profile is very close to linear (as will be shown). Production of TKE is maximum on spring tide and maximum at the bottom decreasing upward into the water column. Peak TKE production is approximately 5×10^{-4} W kg^{-1}.

4.3. Vertical Mixing

[42] From (2) the vertical eddy diffusivity of momentum, A_z, is calculated using measurements of the turbulent stress, $\tau_x/\rho = -\overline{u'w'}$ and vertical shear, $\partial\overline{u}/\partial z$. Sample velocity profiles from maximum flood to maximum ebb on 18 October (year day 291) at the peak of the strong second spring tide are shown in Figure 6. The velocity profiles can be seen to be nearly linear through the portion of the water column resolved by the ADCP with little curvature, thus having a nearly constant shear. The log layer fit below the lowest ADCP bin is also shown. As the shear is nearly constant with depth the profile of A_z over our measurement region follows a near linear distribution with depth. What parabolic shape there is to the A_z profile would occur below the lowest measured ADCP bin where the log layer presumably applies. While stresses are lower on flood than on ebb, shear is less on flood than on ebb.

[43] Significant stresses are mainly generated around the time of maximum flood and ebb at spring tide and these will thus be the times of the greatest vertical mixing. The depth normalized profiles of A_z at the times of maximum flood and ebb at the peak of the spring tide is shown in Figure 6. Like the stresses, the values are greatest near the bed, with values of 1.2×10^{-2} m^2 s^{-1} rapidly decreasing with height above bottom to near zero close to the surface. Flood and ebb values are very similar and both follow the plotted least squares linear fit, which has an $r^2 = 0.81$.

[44] Neap tide stresses are similarly concentrated around times of maximum flood and ebb but, as can be seen in Figure 3, the periods of significant stress generation are much shorter than on spring tide and the high stress region

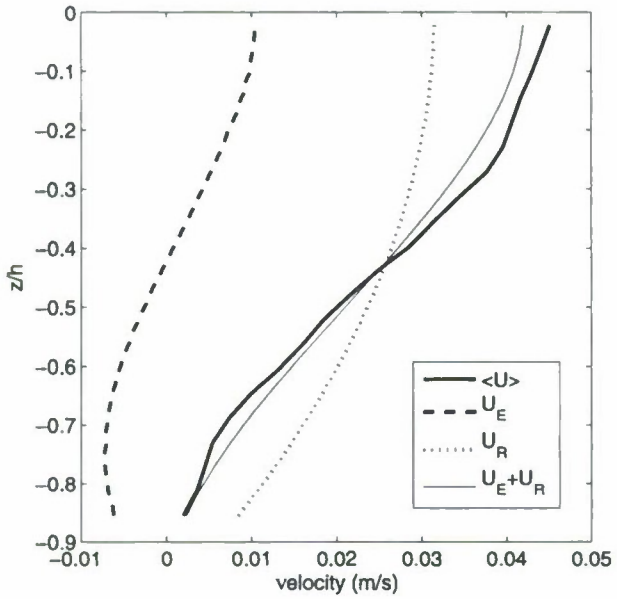

Figure 5. The estuarine circulation and river flow as modeled by equation (21) compared to the measured tidally averaged flow.

does not penetrate nearly as far up into the water column. When the stresses are low, patchy and variable, they do not present a well defined profile in A_z.

[45] As water masses mix through the water column they experience the entire vertical range of mixing levels and thus a depth averaged mixing quantity is approximated by $\widehat{K}_z \sim \widehat{A}_z$ which is shown in Figure 7 (top). Both tidal and fortnightly variability are apparent with values fluctuating strongly during the tidal cycle tied to the generation of stress at the bed. $\widehat{A}_z$ shows M4 variability tied to the two periods of maximum flood and ebb during each lunar day. The 40 h low-pass filtered value of $\widehat{A}_z$, shown by the thick line, varies on a fortnightly time scale being highest on spring tides, centered around year day 277 and 290, in the range of $4–6 \times 10^{-3}$ m^2 s^{-1} and lowest on neap tide, being half to a third of the spring tide values. Even the low values, however, represent significant vertical mixing in this shallow system [*Lewis*, 1997].

[46] Equation (6) is used to calculate the approximate time for complete vertical mixing during a tidal period, using the measured mean water depth (H), and the tidally and depth-averaged value of A_z. This is shown in Figure 7 (bottom) plotted in minutes. Even at its slowest, complete vertical mixing is achieved in slightly over 1 hour and at spring tide takes as little as 20 minutes. This is very much less than the tidal period and implies that the lower Duplin stays well mixed at all times unless acted upon stratifying influences like tidal straining or the estuarine circulation.

4.4. Stratifying Influences

[47] While the rain events and groundwater input could serve to create stratification through straining processes, thus potentially modifying the along channel salt fluxes, the tidal mixing (stirring) serves to homogenize the water column. Figure 8 shows the energetics of stirring and straining according to equation (34) in order to determine if there were times when stratification would become important. The depth averaged turbulent kinetic energy (P) was calculated and a flux Richardson number of $R_f = 0.05$ is assumed. *Di Iorio and Kang* [2007] measure the mixing efficiency Γ in the Altamaha River estuary which is partially to well mixed and show that it is on average 0.05 but can approach the upper limit of 0.2. As expected significant mixing occurs during spring tide which is greater than the stratifying influences of straining.

[48] The straining term is calculated from the measured velocity profiles and the along channel density gradient is calculated from the tidally averaged along channel advection of mass past the mooring as $\partial\rho/\partial x = (-1/U)\partial\rho/\partial t$. The straining effect shows that stratification is created on ebb tide (positive values) and destratification on flood (negative values) with greater effects on ebb owing to its greater flow and shear. Combining the stirring and straining effect, the rate of change of the potential energy anomaly is always negative except for brief periods during neap tide when stratifying influences come into play. These periods of stratification are very short and any stratification that exists at the slack tide will be quickly eroded away during the subsequent flood. If $R_f \sim 0.008$ then there can be stratifying tendencies on every ebb and if $R_f > 0.05$ then no stratification will exist. According to *Geyer et al.* [2008] a distribution of R_f values were obtained in the Merrimack estuary during an ebb tide with a median value of 0.15 and with low values <0.01 during times of weak stratification. As a result the Duplin River can be assumed to be essentially well mixed or weakly stratified only during neap tides.

4.5. Horizontal Transport

[49] The measured salt fluxes per unit width from the various tidal correlations in (16) are shown in Figure 9a as well as their net sum (thick solid line). The largest of these tidal correlation terms is the salt flux into the Duplin due to the correlation between tidal velocity and depth (dashed line). The deeper water on the weaker but longer flood allows more salt to flow in than the shallow waters on the stronger but shorter ebb allow out. The next largest term is a net flux out due to the correlation between velocity and salinity (dotted line) caused by the higher ebb tide velocity exporting salt which has been mixed in on flood. Both of these terms show a strong spring/neap modulation with each approaching zero on neap tide and being greatest on spring. Of the remaining terms the correlation between depth and salinity (thin line) is negated by being multiplied by the very low mean velocity, on the order of ± 1 cm s^{-1}, and the triple correlation is similarly small. The net tidal flux is shown by the thick line as a net flux of salt into the Duplin, where it follows the same strong spring/neap modulation as do its components.

[50] The estimated fluxes due to the estuarine circulation, vertical and transverse shear dispersion calculated from equations (24), (27) and (30), respectively, are shown in Figure 9b. Of these three effects the vertical shear dispersion is the most dominant with values approaching -0.2 m^2/s and longitudinal mixing coefficients $K_{xV} \sim 60$ m^2/s. It should be noted that the linear velocity profile used is actually an overestimation of the kind of shear that actually persists. The effect of the estuarine circulation is a factor of 10^4 smaller. For $K_y = [0.1\ 0.5\ 1.0\ 10]$ m^2/s, cross channel salinity

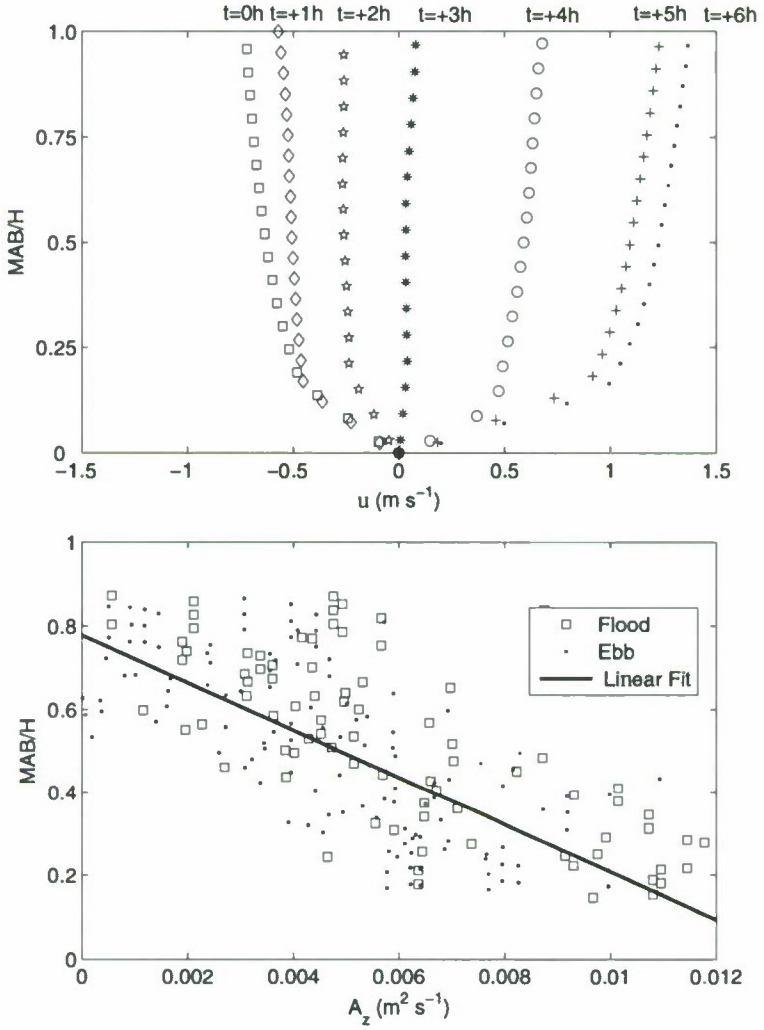

Figure 6. (top) Profiles of along-channel velocity through one tidal cycle from maximum ebb to maximum flood on year day 291. (bottom) Profiles of A_z at maximum ebb and maximum flood, during the times of significant stress generation on spring tide. Depths are normalized with respect to channel depth. The linear fit in the Figure 6 (bottom) has an r^2 of 0.81.

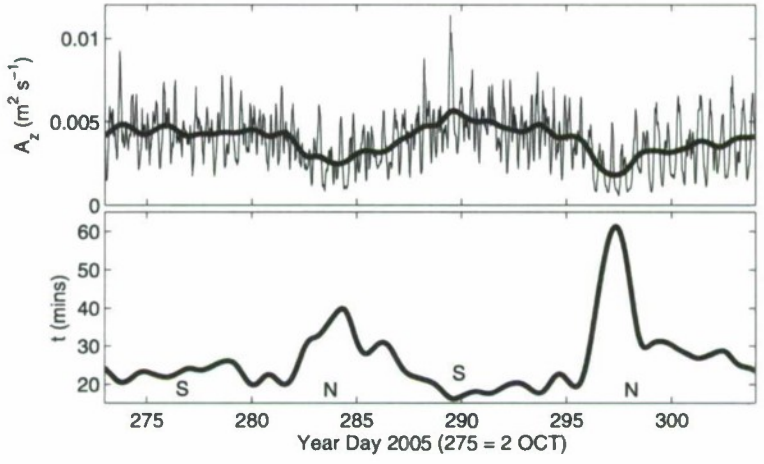

Figure 7. Time series of depth averaged vertical eddy diffusivity of momentum ($\widehat{A_z}$) and vertical mixing time (t) during the deployment period. The thick lines indicate 40 hour low-pass tidally averaged values. The labels S and N indicate times of spring and neap tide, respectively.

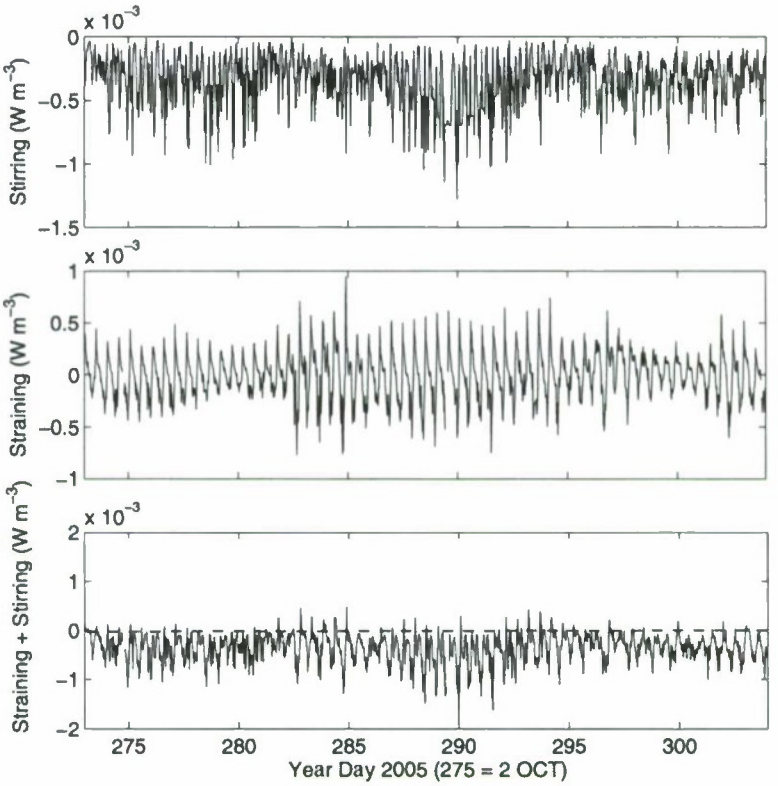

Figure 8. Energetics of (top) mixing and (middle) straining for the destruction (negative values) and creation (positive values) of stratification together with (bottom) their sum.

gradients correspond to a change in salinity of [4.17 0.83 0.42 0.04] in 100 m, respectively. It is unlikely that a cross channel salinity gradient of 4.2 in 100 m exists in this environment and so we limit the value of $K_y > 0.1$ m^2/s and assume that $K_y \sim K_{xV}$. The salt flux from transverse shear dispersion calculated in this way is a factor of 100 smaller than the vertical shear dispersion. If the transverse and vertical shear dispersions are to be of the same order then $K_y \sim 1.0$ m^2/s.

[51] As all these estimated salt fluxes are very much lower than tidal dispersion terms, and thus the effects of possible stratification and hence shear dispersion are judged to be minor players in the long-term salt budget during this time. *Uncles et al.* [1985] also showed that in an estuary of the same scale as the Duplin that the transverse shear dispersion was much smaller than the vertical shear dispersion. The dominant driver of along channel horizontal dispersion is then not shear acting on salinity gradients, but the tidal correlations, which act much more slowly but with greater energy and on larger scales. *Jay and Smith* [1990] outline that barotropic advection of salt dominates over density-driven circulation in maintaining the salt balance in weakly stratified estuaries.

[52] Figure 9e shows the net tidal flux term (dashed line) along with the flux of salt due to residual advection and the change in mean water depth tied to changes in storage volume (thin solid line). Despite the low residual velocity the residual advective term is much greater than the tidal flux term due to the high value of the mean salinity compared to its tidal fluctuations. Net advection varies strongly on a spring/neap cycle showing a pulse-like export of salt on spring tides followed by a weaker, but longer, period of import of salt on neap tides. This pattern, which has been observed before in well mixed to partially stratified estuaries [see, e.g., *Nunes and Lennon*, 1987; *Bowen and Geyer*, 2003] is believed here to be due not only to tidal modulation of upstream dispersive mechanisms but also to variations in the flux of fresh groundwater into the upper/middle Duplin caused by changes in the tidal range on the spring/neap cycle [*Schultz and Ruppel*, 2002].

[53] On neap tide, when the tidal range is small, we hypothesize that little fresh groundwater is pumped into the upper/middle Duplin and thus little pressure is exerted on water in the lower Duplin and residual advection nears zero. Tidal fluxes then bring salt into the lower Duplin and the salinity in this region increases. With the increased tidal range at spring tide, more fresh groundwater is pumped into the upper/middle Duplin which then flows down to the lower Duplin. Residual advection increases as this freshwater mass forces saltier water out of the lower Duplin and salinity decreases as it mixes into the lower Duplin water mass. Tidal dispersion of salt into the lower Duplin increases with the increased tidal energy but it is not enough to overcome the diluting effects of the fresh groundwater. When compared to lower Duplin salinity in Figure 4b the net flux can be seen to closely correlate with changes in the mean salinity in the lower Duplin. The sharp, but short-term, decrease in salinity around year day 280 as well as the lesser, but longer lasting, decrease around year day 290 both correlate with spring tide induced net export as shown in Figure 9d while

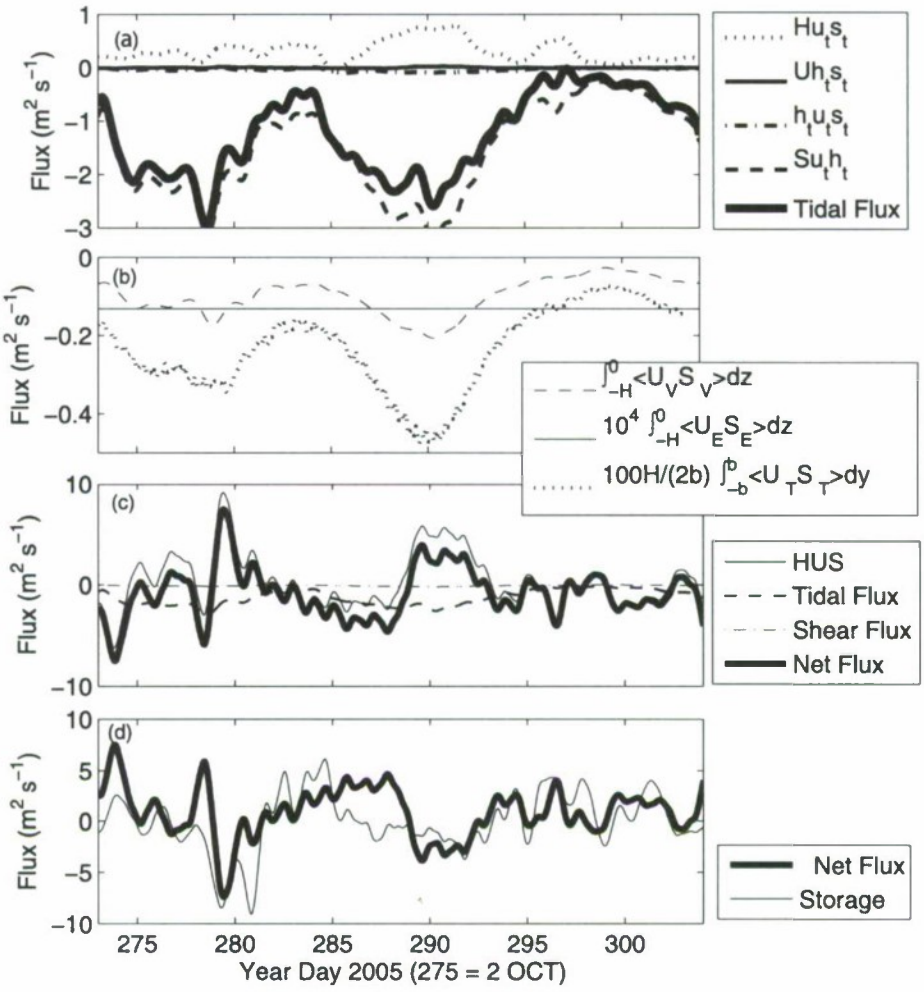

Figure 9. (a) Tidal pumping salt fluxes together with their sum. (b) Estimated salt fluxes due to the estuarine circulation and due to vertical and transverse shear dispersion. (c) Advective and dispersive fluxes and their sum showing the net salt flux per unit width. (d) A comparison between the storage of salt with the net salt flux.

the slow recovery periods correlate with the low net influx of salt on neap tide.

[54] Figure 9d also shows the estimated longitudinally and depth integrated, and tidally averaged storage of salt, per unit width, along with the negative flux of salt, per unit width, past the mooring. While it can be difficult to accurately estimate upstream salt storage [*Simpson et al.*, 2001], a general estimation may be made by combining salinity measurements with an estimate of the time varying volume of water upstream as estimated from tidal height and bathymetry. This estimate will not be precise but will show the general magnitude and trend of the upstream storage of salt.

[55] Both the sign and the shape of the curves compare reasonably well. The general trend of the curves suggest that salinity generally increases during neap tide followed by a decrease in salinity during spring tide. This is believed due to fresh groundwater transported down from the middle Duplin area.

[56] To get an along channel dispersion coefficient K_x for the lower Duplin we normalize the dispersive fluxes (dominated by tidal processes) by the mean water depth and the along channel residual salinity gradient, $\partial S/\partial x$, shown in Figure 10. Figure 10 (top) shows the depth normalized tidal dispersion term from Figure 9 while the Figure 10 (middle) shows the along channel residual salinity gradient, calculated from the tidally averaged along channel advection of salt past the mooring as $\partial S/\partial x = (-1/U)\partial S/\partial t$. The salinity gradient is positive, showing saltier water toward the mouth of the Duplin, with its greatest value on neap tide as decreased tidal energy pumps less salt into the upper reaches of the creek. The ratio of the depth normalized tidal pumping flux with the salinity gradient gives a value for the along channel tidal dispersion coefficient K_x. This is shown in Figure 10 (bottom) and varies strongly on a fortnightly cycle from near 1000 $m^2\ s^{-1}$ on spring tide to close to zero on neap tide with a long-term mean of approximately 500 $m^2\ s^{-1}$.

5. Discussion and Conclusions

[57] We have presented measurements near the mouth of the Duplin River, which is a small and generally vertically

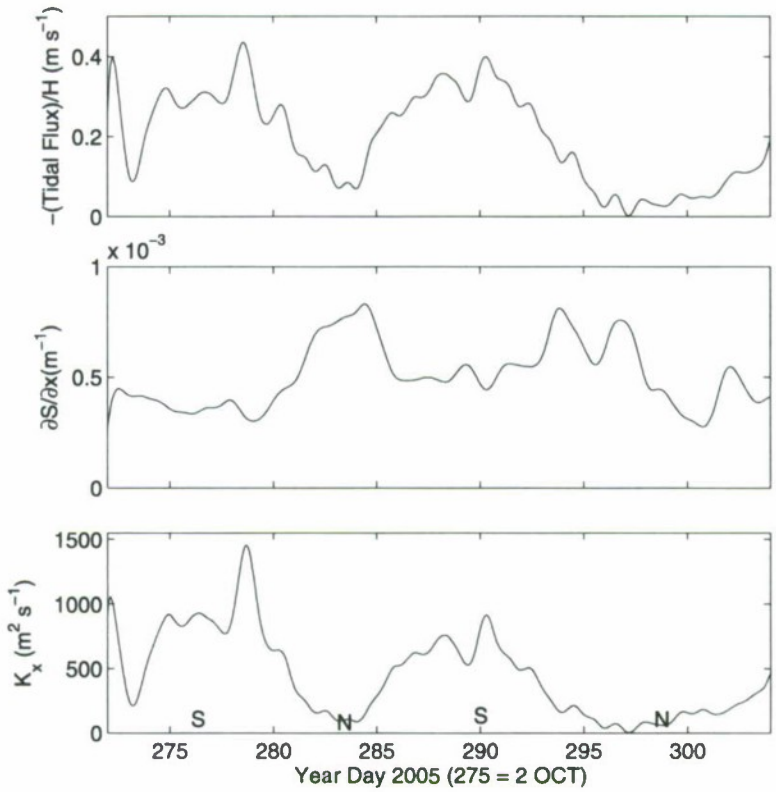

Figure 10. Time series of the dispersive salt fluxes per unit width normalized by mean depth, the along channel salinity gradient, and the resultant along-channel dispersive coefficient (K_x) during the deployment period.

well-mixed tidal creek. This creek system serves as the main conduit between Doboy Sound and the intertidal marshes of the Sapelo Island National Estuarine Research Reserve. The measurements described here directly resolve the vertical velocity structure through most of the 6.5 m mean water depth of the lower Duplin as well as allow the estimation, through the variance method, of the stresses which give rise to vertical mixing. Through salt budget methods we also quantify the along channel tidal dispersion. Spanning a 34 day period, consisting of two spring and two neap tides along with the transitions between these tides, our measurements resolve the wide range of time scales, from turbulent, to tidal and fortnightly, which influence the mixing in these waters.

[58] Estimates of the vertical turbulent stress, τ_x/ρ, show modulation on both tidal and fortnightly frequencies with maximum stress being generated near the bed on maximum flood and ebb at spring tide and linearly decreasing with height above bottom. Neap tide stresses are weaker, concentrated near the bottom and have no variability with depth. Internally generated turbulence plays a larger role near times of slack water with stresses being more broadly distributed through the water column.

[59] Due to the nearly linear profile of velocity with depth and the constant density the Richardson number is almost always much less than the stability criteria of 0.25 and thus from the diffusion of momentum we can approximate the vertical mixing of salt using a turbulent Prandtl scaling of $\sim$1. From this, we estimate that the time for complete vertical mixing varies from 20–30 minutes on spring tide to 40–60 minutes on neap tide and is at all time very much less than the tidal period, thus ensuring that the water column stays well mixed at all times. A comparison of energetics for mixing (R_f = .05) with strained induced periodic stratification show shows that only for brief periods during neap tide can stratification exist.

[60] Tidal dispersive fluxes are, by nature, tidally averaged so we cannot comment on intertidal variability and time scales. These fluxes show a strong spring/neap cycle with maximum upstream dispersive fluxes being found at spring tide while neap tide fluxes approach zero but still being much greater than theoretically predicted vertical and transverse shear effects and effects due to the estuarine circulation. The upstream flux due to the correlation between the tidally varying depth and velocity (tidal wave transport) is the primary driver of along channel dispersion, but it is somewhat counterbalanced by an opposing dispersive flux due to the correlation between tidally varying velocity and salinity. These results are similar to those obtained from *Kaluarachchi et al.* [2003] with the Stokes term being the most significant upstream transport of salt in Newark Bay and Arthur Kill transects but since their model contains only one grid across the channels they could not quantify transverse shear effects. These dispersive salt fluxes are generally overwhelmed by the net advective flux of salt due to the residual flow out of the creek. Residual flows in this environment can be tied to changes in groundwater input, and

changes in rainfall and oceanic forcing from meteorological events.

[61] Interaction between the main along channel flow and the channel edge may result in enhanced along channel dispersion due to the trapping of water in dead zones, side creeks and embayments, and intertidal marshes and mudflats [*Fischer et al.*, 1979]. This water is diverted from the main flow on flood and rejoins it on a different stage of ebb, or on a different ebb altogether, where it mixes with different water masses both creating cross channel gradients and enhancing (or retarding) effective along channel dispersion. Trapping in dead zones, generally eddies associated with channel bends or small embayments and obstructions at the channel edge, is one of the more well studied contributors to enhanced dispersion due to trapping. A number of theoretical and numerical studies, generally in nontidal rivers, [see, e.g., *Purnama*, 1988; *Davis et al.*, 2000; *Davis and Atkinson*, 2000; *Lees et al.*, 2000] have established that in areas of high curvature or channel edge irregularities this can be a major factor in enhancing along channel dispersion, though the exact amount is highly dependent on the local morphology.

[62] As can be seen in Figure 1, our deployment is in an area with a straight channel with few side creeks or irregularities, which results in few dead zones to act on along channel dispersion. The nearest significant side creek, Barn Creek, is located nearly an entire tidal excursion from the mooring location, thus making it unlikely that it plays a role in enhancing dispersion through tidal trapping in the lower Duplin. While there are intertidal marshes bordering the mooring site there is also extensive hard upland, associated with Sapelo Island and several marsh hammocks, or isolated areas of hard upland, which have been shown to greatly reduce the effects of the intertidal areas on local processes, especially as compared to areas further upstream [*McKay and Di Iorio*, 2008]. Due to these considerations it is reasonable to neglect the contributions of channel edge effects and tidal trapping to the along channel dispersion for the lower Duplin.

[63] The net water flux is generally out at spring tide. The increased tidal range on spring tide presumably increases the hydraulic head acting on the aquifer increasing the groundwater flux into the middle and upper Duplin [*Schultz and Ruppel*, 2002]. This increases the downstream pressure gradient and thus increases the net outflow of water. On neap tide, groundwater input into the upper and middle Duplin decreases and tidal pumping, which is no longer opposed as strongly by residual export, brings salt in from Doboy Sound.

[64] The total salt flux due to tidal dispersive and advective fluxes correlates well with the trends in lower Duplin salinity during the deployment period. Examining the net horizontal flux, it becomes apparent that the Duplin shows a net export of salt for a brief period on spring tide, which is followed by a longer period of either net import or near neutral conditions. Salt export is then in a pulsating pattern tied to the fortnightly spring/neap tidal frequency.

[65] **Acknowledgments.** This work was supported by the NSF (OCE-9982133, OCE-0670959) as part of the Georgia Coastal Ecosystems-Long Term Ecological Research (GCE-LTER) project (http://gce-lter.marsci.uga.edu). Thanks go to the captain and crew of the R/V *Savannah* for their assistance in deploying and recovering moorings and to Ken Helm of the UGA Marine Institute for his assistance in maintaining the moorings. Thanks to M. Stacey's review and an anonymous reviewer for comments that led to a much improved paper.

References

Banas, N., B. Hickey, and P. MacCready (2004), Dynamics of Willapa Bay, Washington: A highly unsteady, partially mixed estuary, *J. Phys. Oceanogr.*, *24*, 2413–2427.

Blanton, J., G. Lin, and S. Elston (2002), Tidal current asymmetry in shallow estuaries and tidal creeks, *Cont. Shelf Res.*, *22*, 1731–1743.

Blanton, J., F. Andrade, M. Adelaide-Ferreira, and J. Amft (2007), A digital elevation model of the duplin river intertidal area: Final report submitted to the GCE-LTER Program, technical report, Univ. of Ga., Athens, Ga.

Bowden, K. (1965), Horizontal mixing in the sea due to a shearing current, *J. Fluid Mech.*, *21*(2), 83–95.

Bowen, M., and R. Geyer (2003), Salt transport and the time dependent salt balance of a partially stratified estuary, *J. Geophys. Res.*, *108*(C5), 3158, doi:10.1029/2001JC001231.

Chant, R. (2002), Secondary circulation in a region of flow curvature: Relationship with tidal forcing and river discharge, *J. Geophys. Res.*, *107*(C9), 3131, doi:10.1029/2001JC001082.

Chant, R., R. Geyer, R. Houghton, E. Hunter, and J. Lerczak (2007), Estuarine boundary layer mixing processes: Insights from dye experiments, *J. Phys. Oceanogr.*, *25*, 1859–1877.

Davis, P. M., and T. C. Atkinson (2000), Longitudinal dispersion in natural channels: Part 3. An aggregated dead zone model applied to the River Severn, U.K., *Hydrol. Earth Syst. Sci.*, *4*(3), 373–381.

Davis, P. M., T. C. Atkinson, and T. M. L. Wigley (2000), Longitudinal dispersion in natural channels: Part 2. The roles of shear flow dispersion and dead zones in the River Severn, U.K., *Hydrol. Earth Syst. Sci.*, *4*(3), 355–371.

Di Iorio, D., and A. Gargett (2005), *Sounds in the Sea: From Ocean Acoustics to Acoustical Oceanography*, pp. 500–517, Cambridge Univ. Press, Cambridge, U. K.

Di Iorio, D., and K. Kang (2007), Variations of turbulent flow with river discharge in the Altamaha River estuary, Georgia, *J. Geophys. Res.*, *112*, C05016, doi:10.1029/2006JC003763.

Dronkers, J. (1986), Tidal asymmetry and estuarine morphology, *Neth. J. Sea Res.*, *20*, 117–131.

Dyer, K. (1974), The salt balance in stratified estuaries, *Estuarine Coastal Mar. Sci.*, *2*, 273–281.

Dyer, K. R. (1997), *Estuaries: A Physical Introduction*, John Wiley, Chichester, U. K.

Fischer, H. (1976), Mixing and dispersion in estuaries, *8*, 107–133.

Fischer, H., E. List, R. Koh, J. Imberger, and N. Brooks (1979), *Mixing in Inland and Coastal Waters*, Academic, New York.

Geyer, W., and R. Signell (1992), A reassessment of the role of tidal dispersion in estuaries and bays, *Estuaries*, *15*(2), 97–108.

Geyer, W., M. Scully, and D. Ralson (2008), Quantifying vertical mixing in estuaries, *Environ. Fluid. Mech.*, *8*, 495–509, doi:10.1007/s10652-008-9107-2.

Hansen, D. V. (1965), Currents and mixing in the Columbia River estuary, in *Ocean Science and Ocean Engineering*, vol. 2, pp. 943–955, Mar. Technol. Soc., London.

Hansen, D., and M. Rattray (1965), Gravitational circulation in straits and estuaries, *J. Mar. Res.*, *23*, 104–122.

Imberger, J., T. Berman, R. Christian, E. Sherr, D. Whitney, L. Pomeroy, R. Wiegert, and W. Wiebe (1983), The influence of water motion on the distribution and transport of materials in a salt marsh estuary, *Limnol. Oceanogr.*, *28*(2), 201–214.

Jay, D., and J. Smith (1990), Residual circulation in shallow estuaries: 2. Weakly stratified and partially mixed, narrow estuaries, *J. Geophys. Res.*, *95*, 733–748.

Kaluarachchi, I., M. Bruno, Q. Ahsan, A. Blumberg, and H. Li (2003), Estimating the volume and salt fluxes through the Arthur Kill and the Kill Van Kull, *ASCE Conf. Proc.*, *118*, 225–235, doi:10.1061/40685(2003)225.

Kjerfve, B. (1973), Volume transport, salinity distribution and net circulation in the Duplin estuary, Georgia, *Tech. Rep. ERC-0273*, Univ. of Ga., Sapelo Island, Ga.

Kjerfve, B. (1986), Circulation and salt flux in a well mixed estuary, in *Physcis of Shallow Estuaries and Bays*, edited by J. van de Kreeke, pp. 22–29, Springer, Berlin.

Lees, M. J., L. A. Camacho, and S. Chapra (2000), On the relationship of transient storage and aggregated dead zone models of longitudinal solute transport in streams, *Water Resour. Res.*, *36*(1), 213–224.

Lewis, R. (1997), *Dispersion in Estuaries and Coastal Waters*, John Wiley, Chichester, U. K.

Lohrman, A., B. Hackett, and L. Roed (1990), High resolution measurements of turbulence, velocity, and stress uding a pulse-to-pulse coherent SONAR, *J. Atmos. Oceanic Technol.*, *7*, 19–37.

Lu, Y., and R. Lueck (1999), Using a broadband ADCP in a tidal channel. Part II: Turbulence, *J. Atmos. Oceanic Technol.*, *16*, 1568–1579.
McKay, P. (2008), Temporal and spatial variability of transport and mixing using heat and salt in the Duplin River, Georgia, Ph.D. thesis, Univ. of Ga., Athens, Ga.
McKay, P., and D. Di Iorio (2008), Heat budget for a shallow, sinuous salt marsh estuary, *Cont. Shelf Res.*, *28*(4), 1740–1753.
Medeiros, C., and B. Kjerfve (2005), Longitudinal salt and sediment fluxes in a tropical estuary: Itimaraca, Brazil, *J. Coastal Res.*, *21*, 751–758.
Nunes, R., and G. Lennon (1987), Episodic stratification and gravity currents in a marine environment of modulated turbulence, *J. Geophys. Res.*, *92*, 5465–5480.
Peters, H. (1997), Observations of stratified turbulent mixing in an estuary: Neap-to-spring variations during high river flow, *Estuarine Coastal Shelf Sci.*, *45*, 69–88.
Pritchard, D. (1952), Estuarine hydrography, *Adv. Geophys.*, *1*, 242–280.
Pritchard, D. (1954), A study of the salt balance in a coastal plain estuary, *J. Mar. Res.*, *13*, 133–144.
Pumama, A. (1988), The effect of dead zones on longitudinal dispersion in streams, *J. Fluid Mech.*, *186*, 351–377.
Ragotzkie, R., and R. Bryson (1955), Hydrography of the Duplin River, Sapelo Island, Georgia, *Bull. Mar. Sci. Gulf Caribb.*, *5*, 297–314.
Rattray, M., and J. Dworski (1980), Comparison of methods for analysis of the transverse and vertical contributions to the longitudinal advective salt flux in estuaries, *Estuarine Coastal Mar. Sci.*, *11*, 515–536.
Rippeth, T., E. Williams, and J. Simpson (2002), Reynolds stress and turbulent energy production in a tidal channel, *J. Phys. Oceanogr.*, *32*, 1242–1251.
Schultz, G., and C. Ruppel (2002), Constraints on hydraulic parameters and implications for groundwater flux across the upland-estuary interface, *J. Hydrol.*, *260*, 255–269.
Simpson, J. (1994), *Sea Breeze and Local Winds*, Cambridge Univ. Press, Cambridge, U. K.
Simpson, J., J. Brown, J. Matthews, and G. Allen (1990), Tidal straining, density currents, and stirring in the control of estuarine stratification, *Estuaries*, *13*, 125–132.
Simpson, J., R. Vennell, and A. Souza (2001), The salt fluxes in a tidally energetic estuary, *Estuarine Coastal Shelf Sci.*, *52*, 131–142.
Simpson, J., E. Williams, L. Brasseur, and J. Brubaker (2005), The impact of tidal straining on the cycle of turbulence in a partially stratified estuary, *Cont. Shelf Res.*, *25*, 51–64.
Souza, A., and J. Simpson (1997), Controls on stratification in teh Rhine ROFI system, *J. Mar. Syst.*, *12*, 311–323.
Stacey, M., S. Monismith, and J. Burau (1999a), Observations of turbulence in a partially stratified estuary, *J. Phys. Oceanogr.*, *29*, 1950–1970.
Stacey, M., S. Monismith, and J. Burau (1999b), Measurements of Reynolds stress profiles in unstratified tidal flow, *J. Geophys. Res.*, *104*, 10,933–10,949.
Uncles, R., R. Elliott, and S. Weston (1985), Dispersion of salt and suspended sediment in a partly mixed estuary, *Estuaries*, *8*, 256–269.
Verity, P. G., J. A. Yoder, S. S. Bishop, J. R. Nelson, D. B. Craven, J. O. Blanton, C. Y. Robertson, and C. R. Trunzo (1993), Composition, productivity and nutrient chemistry of a costal ocean plankton food web, *Cont. Shelf Res.*, *13*, 741–776.
Wiegert, R. G., M. Alber, C. Alexander, J. O. Blanton, A. Chalmers, R. E. Hodson, M. A. Moran, L. R. Pomeroy, and W. J. Wiebe (1999), The Georgia rivers land margin ecosystem research program, *Limnologica*, *29*, 286–292.
Williams, E., and J. Simpson (2004), Uncertainties in estimates of Reynolds stress and TKE production rate using the ADCP variance method, *J. Atmos. Oceanic Technol.*, *21*, 347–357.

D. Di Iorio, Department of Marine Sciences, University of Georgia, Athens, GA 30602, USA. (daniela@uga.edu)
P. McKay, Naval Research Laboratory, Code 7322, Stennis Space Center, MS 39529-5004, USA. (paul.mckay.ctr@nrlssc.navy.mil)